5.5 PRE- AND POST- SEA BREEZE FRONTAL LINES - A MESO-γ SCALE ANALYSIS OVER SOUTH ISRAEL

Pinhas Alpert *

Department of Geophysics and Planetary Sciences, Tel Aviv University, Tel Aviv 69978, ISRAEL

Michal Rabinovich- Hadar

Department of Geophysics and Planetary Sciences, Tel Aviv University, Tel Aviv 69978, ISRAEL

1. INTRODUCTION

A vast literature exists on the characteristics of the sea-breeze front (SBF, km) based on observations, e.g. Atkinson (1981), Simpson (1994). Until the 1940's the focus was on surface or near-surface measurements and since then the upper level circulation of the SBF was also explored with the aid of balloons, airplanes, radar, satellite, Doppler-radar and more recently theoretical and/or numerical models, e.g. Kimble (1946), Haurwitz (1947), Pearce (1955), Estoque (1962), Neumann and Mahrer (1971, 1974), Simpson et al. (1977), Alpert et al. (1982), Wakimoto and Atkins (1994). A more recent summary of the sea breeze and local winds is given by Simpson (1994).

The SBF was basically identified with change in wind direction, increase of wind speed, drop in temperature and increase of the humidity associated with the arrival of the relatively cool and humid sea airmass, e.g. Atkinson (1981, Fig. 59). Or, alternatively, in the drop of virtual temperature, increase of the dew point or the equivalent potential temperature, Wakimoto and Atkins (1993). The intensity of these changes varies in place, season and latitude. In India and Israel, for instance, the average SBF wind speed is 4-5 ms^{-1} and temperature drop is 1-5°C.   Normally, the northern hemispheric rotation of the wind direction is clockwise due to the Coriolis force as shown by Neumann (1977). In some locations, however, rotation could be in the anti-clockwise sense (Staley, 1957; Alpert et al. 1984), and Kusuda and Alpert (1983) have attributed this to an additional pressure-gradient forcing out of phase with that of the SBF sometimes acting even parallel to the seashore line, like due to topography.

Several studies focused on the horizontal and vertical propagation of the SBF as in Australia (Clarke, 1955), in California (Schroeder et al., 1967) or in England (Simpson et al, 1977). Others investigated the effects of the synoptic flow, e.g. Estoque (1962), Helmis et al. (1987), Arritt (1993), and Wakimoto and Atkins (1993).

* *Corresponding author address:* Professor Pinhas Alpert, Department of Geophysics and Planetary Sciences, Tel-Aviv University, Tel-Aviv 69978, ISRAEL; e-mail: pinhas@cyclone.tau.ac.il

In Israel, a number of pioneer theoretical studies on the SBF were performed by Neumann and Mahrer (1971, 1972), Neumann (1977), Alpert et al. (1982), Segal et al. (1985). A few studies, however, were oriented to observational analyses.   Skibin and Hod (1979) performed subjective analyses of mesoscale flow pattern over north Israel. Alpert and Getenio (1988) and Alpert (1988) have combined surface wind observations with 3-D and 2-D model predictions in order to obtain the best description of the mesoscale summer flow characteristics in Israel.   These observational studies, however, have not gone below typically 3-h time intervals of the observed synoptic data.

The purpose of the present study is to first attempt to develop surface-based objective criteria for detection of SBF with a high temporal resolution having a 5 min time interval data. Second, to explore the meso-γ scale characteristics of the summer SBF in Israel employing both a high temporal resolution (5 min) and a unique spatial (12 stations over 400 km^2) automatic net of environmental stations. In particular, attention is given to the evidence presented here for the existence of pre- and post SBF lines over the south coast of Israel and their possible relationship with earlier theoretical prediction on the SBF forerunners by Geisler and Bretherton (1969).

2. METEOROLOGY OF OBSERVATIONAL ANALYSIS

2.1 Description of stations and data

Figure 1 shows a map of the study area over the south-east Mediterranean Coast, Israel and the 14 meteorological stations. This makes a dense net over an area strip of 40 km long and 20 km width. For 12 of the stations the average area per station is only about 33 km^2. Except the two northernmost stations (i.e. Ash-Bazan and B. Gamliel) the stations are for environmentally monitoring of the air downstream of the towns of Ashdod (136N, 119E) and Ashkelon (119N, 109E) where coal-based electric power plants are operating. Several years ago the air-quality was exceptionally low particularly downstream of Ashdod and the recent use of low-sulphur gasoline in prone synoptic situations based on advanced warnings has much improved the air-quality over this area.   The stations automatically record wind speed and intensity as well as temperature continuously and 5 min averages are carried out.   In the stations Ashdod, Ashkelon and K. Gat

additional parameters like humidity, pressure, global radiation and rainfall are also measured. Pollutants concentrations of SO_2, No_x, NO and O_3 are also being measured at all the environmental stations.

The two northernmost stations do not measure pollutants but meteorological fields at few levels. At Ashdod-Bazan tower (139N, 120E) wind, temperature and humidity are taken at 2, 10 and 60 m while in B. Gamliel tower (author's P.A. house 141N, 128E) temperature measurements at 0.5, 2 and 10 m are taken every 10 min.

Meteorological parameters that were found consistently exceptional or suspicious with erroneous reports were not employed here for the comparison study. For instance, the humidity at Ashdod was consistently too low. Reasons for that may be improper positioning or non-standard location or inaccurate calibration of the instrument. But, they may still be used sometimes, to identify the SBF arrival in the method described next.
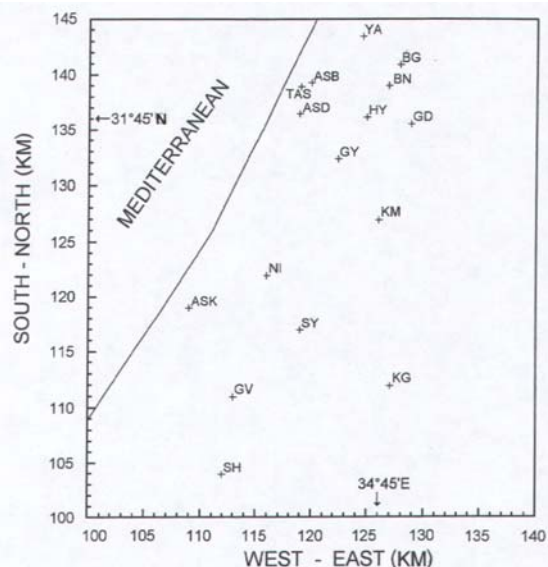

Figure 1 Map of area and all the surface stations. Axis numbers are in km according to local geographic coordinates.

2.2 Data analysis methodology

The summer day of the 20 July 1993 was chosen for preliminary analysis since most of the data was available. It was later found to present a nicely developed SBF with weak synoptic forcing. The dominant synoptic summer pattern is a subtropical high over Israel along with a Persian trough over the north with typical northwest-west winds of about 2-5 ms^{-1}, Alpert et al. (1992). Early morning low-level stratocumulus clouds frequently form, but quickly dissipate because of the strong subsidence.

The original 5 min average data was found highly fluctuating reflecting the higher turbulent daily data

associated with the vigorous large eddies typical for clear days with strong solar irradiation. Hence five and seven points running averages (20 and 30 min respectively) were found useful for the detection of the SBF by partly smoothing the turbulence. Figs. 2-4a,b show the original 5 min data and the 20 min (in brevity, AVG5 indicating 5-point average) averaged time-series for wind direction (Figs. 2a,b) wind speed (Figs. 3a,b) and temperature (Figs. 4a,b), respectively, for the station Nir-Israel [NI, 122N, 116E, Fig. 1]. The original wind direction in Fig. 2a possesses high variability while the 5-point smoothing in Fig. 2b clearly shows a steady and sharp clockwise wind turning between 1025 to 1045 LT from southerly 190° to westerly 260°. Similarly, the smoothed wind speed in Fig. 3b indicates a sharp increasing trend from 1.5 to 3.5 ms^{-1} during 1045 to 1115 LT. The original temperature time series, Fig. 5a, shows several times where the temperature stabilizes or even drops, i.e. at 0850, 0950, 1035, 1055 h LT, but the AVG5 plot, Fig. 4b, emphasizes the 1105 h clear change in the temperature trend. From this time onward for about 50 min the average temperature drops in spite of the continuing increase of the solar heating, clearly indicating the SBF arrival. The seven-point smoothing was also analyzed (Rabinovich, 1995) but not found necessary for the further analysis. The humidity variations were available only in 4 stations and will be discussed later.
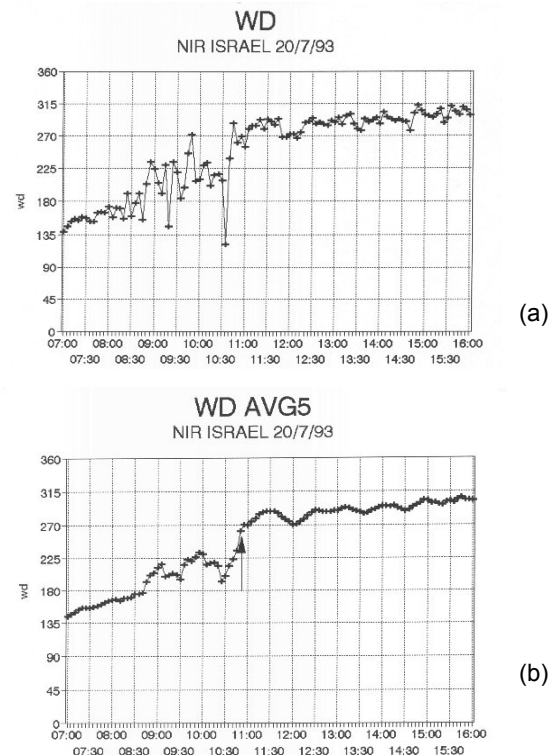

Figure 2a, b Time series of wind direction (WD in degrees) in Nir Israel (NI) on 20 July 1993. (a) Basic data at 5 min interval (b) 5 points running average indicated as AVG5. Arrow indicates SBF passage (see text). Abscissa indicates local time, which is 2 h ahead of UTC (LT=UTC+2h). With summer time LT is 3 h ahead of UTC time.
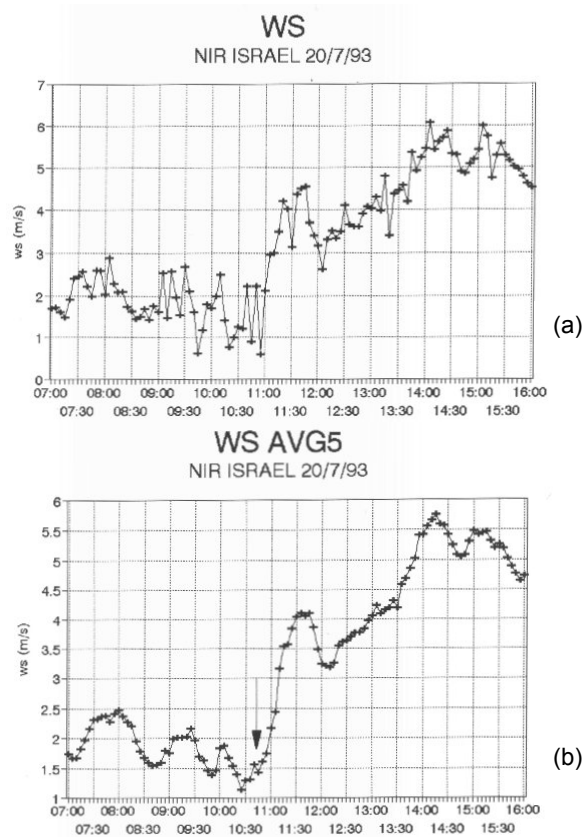
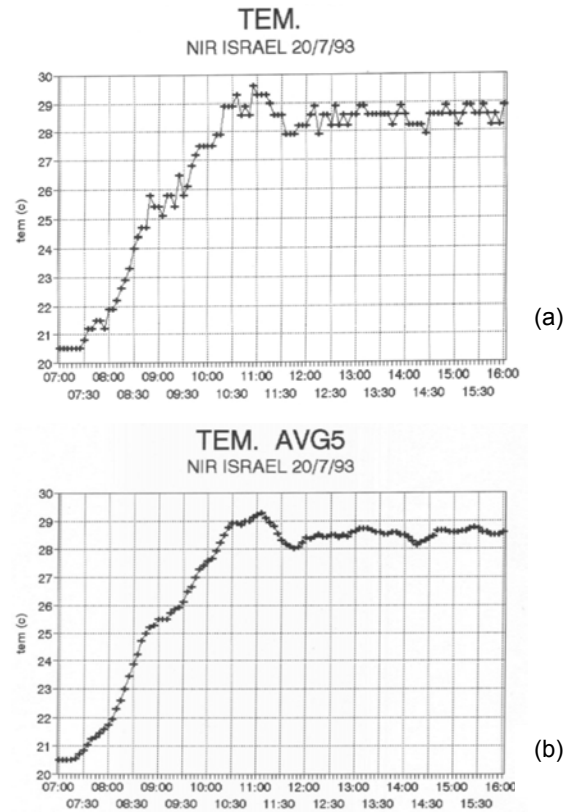**Figure 3 a, b** As in 2 but for wind speed (WS) in ms^{-1}.

Figure 4a, b As in 2 but for temperature (^{o}C).

3. CRITERIA FOR THE SBF

3.1 *Formulation of objective criteria for SBF arrival*

A computer program was written in order to objectively calculate the SBF arrival points along with a subjective inspection of the results for a period of 10 days during the summer for all the stations. The SBF arrival is accompanied by clockwise wind rotation, wind speed increase, temperature drop and humidity increases. But, not all these signs appear in unison since their expression depends on the SBF intensity and its stage of evolution, i.e. near the coast or farther inland. The decision whether to take the beginning or end of the variation for a specific field was based on an attempt to fit the different SBF arrival times based on the various parameters into the shortest time-span. A similar choice was done by Chiba (1993). Consequently, in all the parameters except the wind direction, the SBF time was chosen to be the beginning of the change. This suggests (as discussed later) that the wind direction is a particularly sensitive parameter.

At the end of the inspection process the following criteria for SBF arrival were chosen based on the AVG5 data:

I. <u>Wind direction</u>: End of clockwise rotation (CWR) of at least 45 deg within 15 min. In case such a wind turning was not found the largest CWR which extended at least 15 min was chosen.

II. <u>Wind speed</u>: Beginning of a continuous wind increase of at least 1.5 ms^{-1} within 35 min. In case such a temporal gradient was not found, the largest increase that extended at least 25 min was chosen.

III. <u>Temperature</u>: Beginning of decrease or stabilizing (stops increasing) for at least 15 min.

IV. <u>Relative humidity</u>: Beginning of increase or stabilizing for at least 15 min (see Ch. 3.3).

V. <u>Turbulence intensity</u>: Point of maximum turbulence intensity, see next section.

For the aforementioned example of Nir Israel on 20 July 1993 criteria (I-III) yield the SBF arrival times of 1045, 1045 and 1100 respectively. Several problems related to the aforementioned criteria will be discussed later in Ch. 3.4.

3.2 Turbulence intensity as an additional criterion

Since most stations had only 3 regularly observed parameters, i.e. wind direction, wind speed and temperature, it was found useful to introduce an additional parameter, the turbulence intensity or gustiness.

Turbulence intensity may be defined as the ratio between the wind speed standard deviation, $\sigma = \sqrt{\overline{v'^2}}$, and the average wind speed $\overline{v}$, e.g. Alpert and Eppel (1985),

$$G = \frac{\sqrt{\overline{v'}}}{\overline{v}} = \frac{\sigma}{\overline{v}}, \qquad (1)$$

Where v' is the instantaneous or turbulent wind taken as the 5 min basic measurement. It is also sometimes entitled as the gustiness, e.g. Glossary (1959). It was calculated at each time based on the 7-point measurements (equivalent to 30 min time period) around the pertinent time.

Fig. 5 illustrates the turbulence intensity (G) time series for the station Nir-Israel as in Figs. 2-4. It shows a steady increase of G from about 0930 and the absolute maximum is reached at exactly 1100 which fits well the change in wind direction (Fig. 2b, 1045h) the change in wind intensity (Fig. 3b, 1045h) and the decrease in temperature (Fig. 4c, 1100h).

Hence, the 5th criterion for the SBF became the absolute maximum in gustiness. This additional criterion was inspected for all stations in the same days and was

found very useful in the objective computerized decision-making in some problematic situations (see Ch. 3.4).
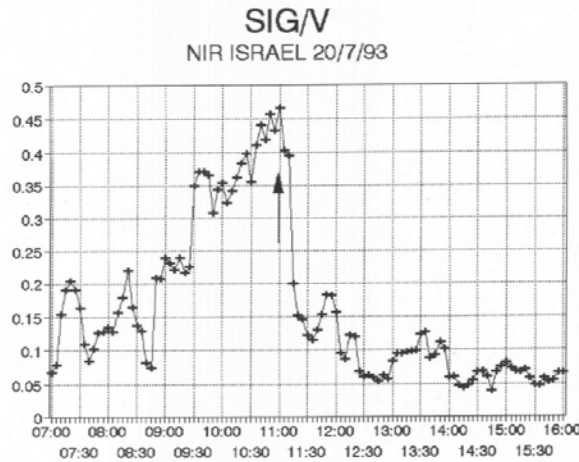

Figure 5 As in Fig. 2 but for turbulence intensity or gustiness, G.

3.3 Examination of the humidity criterion (IV)

Obviously, the relative humidity (i.e. RH) is closely associated with the temperature, as for instance, the RH may increase due to a temperature drop without any humidity increase. Consequently, the specific humidity, q, was calculated based on the following formula, e.g. Rogers and Yau (1989),

$$q = \frac{RH}{100} \bullet \frac{R}{R_v} \frac{1}{p} A e^{-B/T} \qquad (2)$$

where $A = 2.53 \cdot 10^7$ hPa, $B = 5420$ K, T temperature in K, $R = 287$ J kg^{-1}K^{-1} gas constant, $R_v = 461$ J kg^{-1}K^{-1} gas constant for water vapor and p pressure in hPa.

Results with specific humidities (q) were found not much different but sometimes q serves as a better indicator for the SBF arrival. For instance, Figs. 6a-c show both q and RH at the Ashdod, Ashkelon and K. Gat stations (ASD, ASK and KG, Fig. 1) respectively. The q scale in g kg^{-1} is on the left while the RH (%) scale is on the right. In Ashdod (Fig. 6a) the tendencies are similar; both show small increase at 0730 LT (probably part of the break in the nocturnal surface inversion) with a more significant increase at 0855 h associated with the SBF arrival (see later). In Ashkelon (Fig. 6b), however, the specific humidities increase sharply early in morning while RH stay at the maximum, of 100%. At 1000-1030 there is a sharp decrease in the specific humidity and the RH, which is probably related to break in the nocturnal inversion, e.g. Segal et al (1992). Only at 1050-1100h there is an increase in both RH and q parameters which fits the other SBF criteria for the Ashkelon station (not shown). Similar patterns are found in Kiryat Gat, Fig. 6c. Here, however, the SBF arrival at 1200 is recognized by a much sharper increase in the specific humidities as well as the RH.
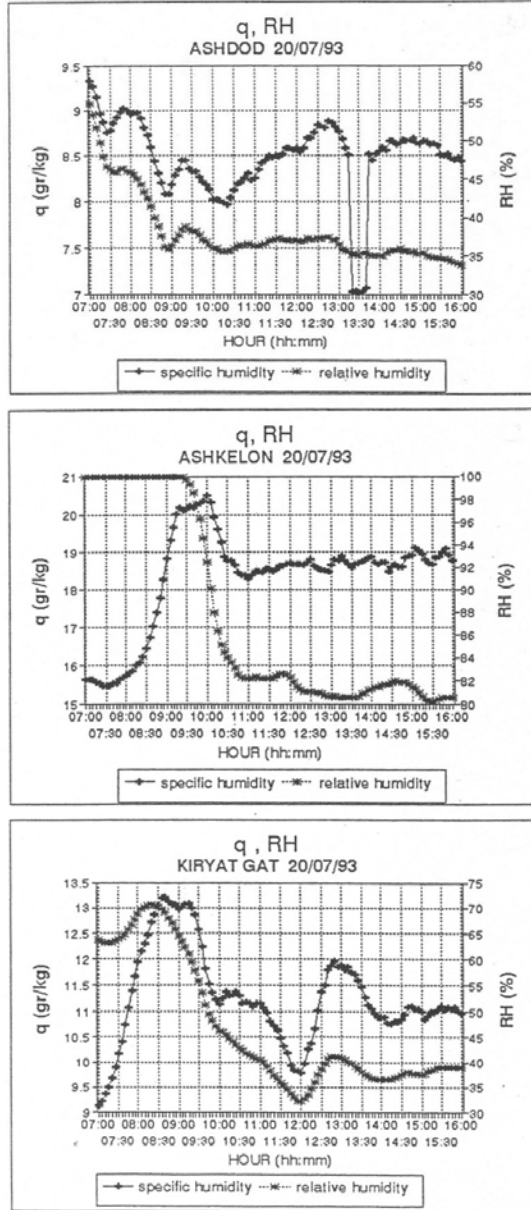
(a)

(b)

(c)

Figure 6a- c Time series of specific humidity, q (++++), relative humidity, RH (*-*-*) at (a) Ashdod (b) Ashkelon and (c) Kiryat Gat (ASD, ASK and KG in Fig. 1) for 20 July 1993. Scale for q is on the left and scale for RH on the right.

3.4 *Objective detection of the SBF- associated problems*

At each station four (or 5 when humidity was available) SBF arrival times according to the aforementioned 4 (5) criteria, were defined. If all times were within one hour the earliest time was chosen. Figs. 7a-d, for instance, show the corresponding 4 figures for the station GVARAAM; humidity was not available. According to the wind direction (criterion I), SBF arrival was at 1050h, Fig. 7a. Similarly, the temperature, wind speed and gustiness (Figs. 7b,c,d) yielded the times of

1120, 1105 and 1120 LT respectively. Hence, the chosen SBF arrival time at GVARAAM was 1050h.
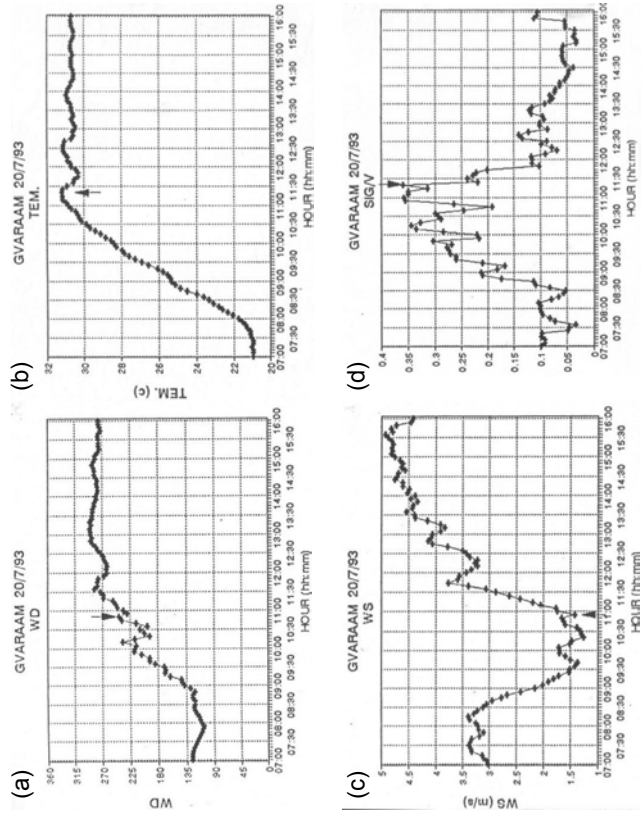

(b)

(d)

(a)

(c)

Figure 7a-d Time series at GVARAAM (GV) for (a) wind direction (deg) (b) temperature (^{o}C), (c) wind speed (ms^{-1}) and (d) gustiness G. All for 20 July 1993.

In computerizing all the criteria there are several problems besides those that are related to the quality of the data. First, the gustiness parameter may become large even without considerable fluctuations such as when the average wind is very weak ($\overline{V}$ close to zero in Eq. 1), along with even a weak change in a wind speed. Hence, there are gustiness (G) peaks that may not be related to the SBF.

Second, in some stations in some days the wind veering is too slow to obey criterion I. This was the reason for modifying criterion I to the largest clockwise rotation (CWR) which was found steady within 15 min. For very gradual turning such a criterion may not be useful. In some cases the other criterions were also questionable but frequently when only this wind veering difficulty occurred, it may have been related to an instrumental problem.

Third, in summer, wind turning was indeed always clockwise but in the transition seasons where anti-clockwise rotation may have occurred (due to change in the synoptic forcing), the criterion was modified to the time when turning to the west or northwest sector has happened.

A fourth problem relates to effect of cloudiness, since even a small cloud fraction may significantly influence the screen temperature, e.g., Segal and Feingold (1993). With heavier cloudiness, the other criterions may also be strongly affected. But, only 4 stations carry global radiation from which cloudiness was inferred. Hence, the analysis in cloudy days became complicated and such days, which are rare over our study region of south Israel, were filtered out.

Sometimes, a retrograding sea breeze was observed. This may happen when the sea breeze opposes the synoptic gradients but is quiet rare during summer. Such a winter case, however, was simulated and discussed by Alpert et al. (1988). Here, focus was given to summer cases where these situations are extremely rare.

In cases where two parameters supported one arrival time and the other two points another time, both arrival times were plotted. Finally, SBF arrival times for all stations were plotted over a geographic map and isochrones for SBF arrival time were drawn. Fig. 8, for instance, shows the SBF arrival time isochrones for the 20 July 1993. It shows that the SBF enters first over the northern section at about 0830 LT. Rate of SBF propagation inland increases as the SBF enters inland and will be discussed.
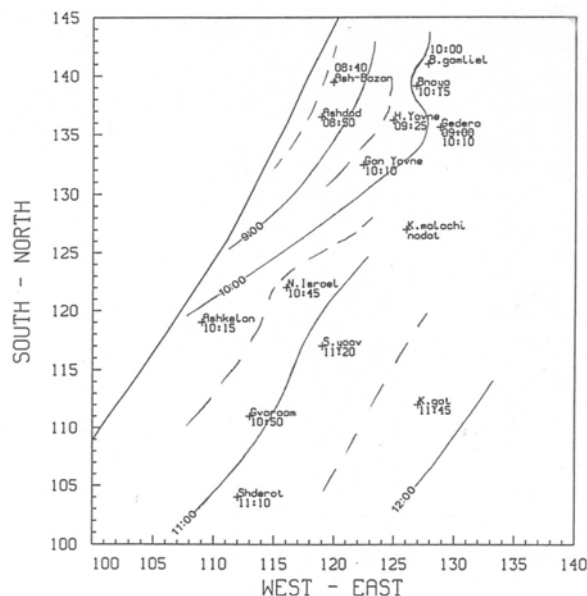

Figure 8 The SBF arrival time isochrones for the 20 July 1993. Full (dashed) lines for full (half-dashed) hour isochrones. Times below each station   indicate SBF passage time (s) according to the criteria derived.

4. CHARACTERISTIC OF THE SUMMER SEA BREEZE FRONTS AND THEIR PRE- AND POST-LINES

4.1 *Observations for a specific day*

In the daily examples shown so far one may notice additional weaker lines ahead from and in the wake of SBF. For instance, in Nir Israel, Figs. 2-4b, and Fig. 5 besides the identified dominant SBF at 1045-1100 there exists a pre-frontal line at about 0840 and 0940-0950 LT clearly noticed by the wind direction (Fig. 2b), the wind speed (Fig. 3b) and by the secondary maxima in the gustiness (Fig. 5). They are clearly noticed in the non-averaged temperature (Fig. 4a) but also as breaks in the steep slope of the AVG5 temperature increase at 0840 and 0950 LT (Fig. 4b).

A post-front can also be identified at about 1h after the passage of the primary SBF, i.e. at about 1210 LT. The corresponding exact times are 1230 (WD), 1210 (WS), 1215 (T) and 1155 or 1215 (G). Similarly, at GVARAAM one can clearly notice additional pre- and post-frontal line. Since these lines are weaker than the dominant SBF they may sometimes be more easily noticed in the non-averaged fields, and the aforementioned criteria need to be less stringent.

Are these lines just turbulence due to the large-eddies or real pre- and post-lines dynamically associated with the SBF? Do they carry on any consistent features?

4.2 *Observations for periods of several days*

This will be examined next by inspecting the SBF character over a period of 8 consecutive days in 1993 (18-25 July) and also for 9 d in 1994 (20-28 July). The averaging for the 8 or 9d was performed every 5 min at each station and for all the parameters. We may consider this as a semi-climatological analysis of the July SBF. It is absolutely striking to indicate that besides the primary SBF, there are indeed pre- and post SBF converging lines that are clearly noticed and are supported by either all the parameters or some of them. The pre-SBF lines found here may be related to the forerunners predicted in the theoretical study of Geisher and Bretherhon (1969), but we are not aware of any reference for the post SBF – frontal lines. Before presenting the results we should notice that, first, the convergence lines are strongly noticed by the gustiness G. Second, since this is a multi-day average for which the exact criteria defined earlier for a single day cannot strictly apply but the search for the SBF features will be done similarly. Also, a small time correction of 5-7 min due to the progression of the sunrise time in late July through the 8 or 9d was not applied. Obviously, not all the parameters supported each converging front-line but they became more definite with the increasing number of parameters that supported its existence.

In addition we have calculated the inter-daily standard deviation of the wind direction SIGD for each station. We do expect to have a stronger SIGD at times

straddling around the expected SBF arrival, as indeed observed, e.g. Fig. 2a for Nir-Israel. But, this time interval with maximum variability is also influenced by both the inter-daily synoptic variations, though small, and the aforementioned gradual change in the sun angle.

Fig. 9 presents the time-series for WD, WS, SIG/V, TEM and RH in Ashkelon for July 1993 and 1994 for 8 and 9d averages, respectively. The interdaily wind direction standard deviation SIGD is plotted on the top panel for the WD series (the line at the bottom of 9a left and right). The two panels from top down are: WD (and SIGD), WS, SIG/V, TEM and RH; left panel for 1993 and right for 1994. Following the detection criteria discussed in Sec 3.about four lines of convergence can be identified by some or all of these criteria. At around 0720 LT, about 1-2h past sunrise we can notice a small peak in the turbulence intensity, SIG/V; also found in SIGD and WS and probably indicating the break of the aforementioned early morning surface inversion. The more pronounced first convergence line, probably pre-frontal, is noticed at about 0815-0850. In 1993 (left panel), it is noticed by the significant maximum of SIG/V at 0835 and some strengthening of the wind speed (WS) at 0825. In 1994, the SIG/V maximum is at 0815 and 0855, strengthen of WS at 0815 and light drop of TEM at 0850.

The second most noticeable convergence line can be identified at 0940-0950 as the main SBF. It is clearly noticed by SIG/V, WS, WD, TEM and even some weakening in the sharp decrease of the relative humidity, RH.

The third converging line - post frontal - is found at 1010 -1025 in both 1993 and 1994 panels, and is strongly supported by the relative humidity and temperature (RH and TEM) but can also be noticed in SIG/V and WS.

The fact that the three converging lines including the pre and post SBF do appear even in 8 or 9 summer days averages in two years support the significance of the pre and post SBF lines; lines that remained so far nearly untouched in the extensive literature on the sea-breezes.

5. SUMMARY

This work presents a meso-γ scale station analysis of the sea breezes over the south coastal plane of Israel employing high spatial and temporal resolutions.

We have formulated objective criteria for the SBF passage based on wind speed/direction, temperature and relative humidity. This suggests the option to realize a computer operational warning system as for instance in relation with pollutant dispersion. The paper focuses on summer cases where the synoptic forcing is quiet steady, Alpert et al. (1992), therefore allowing a very detailed inspection of the SBF characteristics.

The criterions included, fast veering of the wind, significant increase of wind speed, temperature decrease, humidity increase and maximum in the turbulence intensity. The criteria were found reliable on clear days. The most convenient criteria for the SBF were found the specific humidity, temperature and turbulence intensity.

Except for the primary SBF we have found pre/post frontal lines. This finding is preliminary and was not reported earlier as a steady phenomena for many summer days. It is important for pollutant transport, human comfort and in general for a more fundamental understanding of the SB phenomenon. There are some theories suggesting possible mechanisms to explain secondary frontal lines like the Geisler and Bretherton (1969) forerunners or the Sha et al (1991) on Kelvin-Helmholz waves past the SBF. In presenting our pre – and post – frontal lines analysis to C. Ramis it was pointed out that a trace of post – SBF line can also be noticed in Mallorca observations in Spain, Ramis et al. (1990).

Our preliminary study suggests that a most convenient field to identify the secondary SBF is the turbulence intensity followed by wind speed and temperature mainly for the post-frontal lines. It is difficult to notice any significant wind veering associated with the secondary lines.
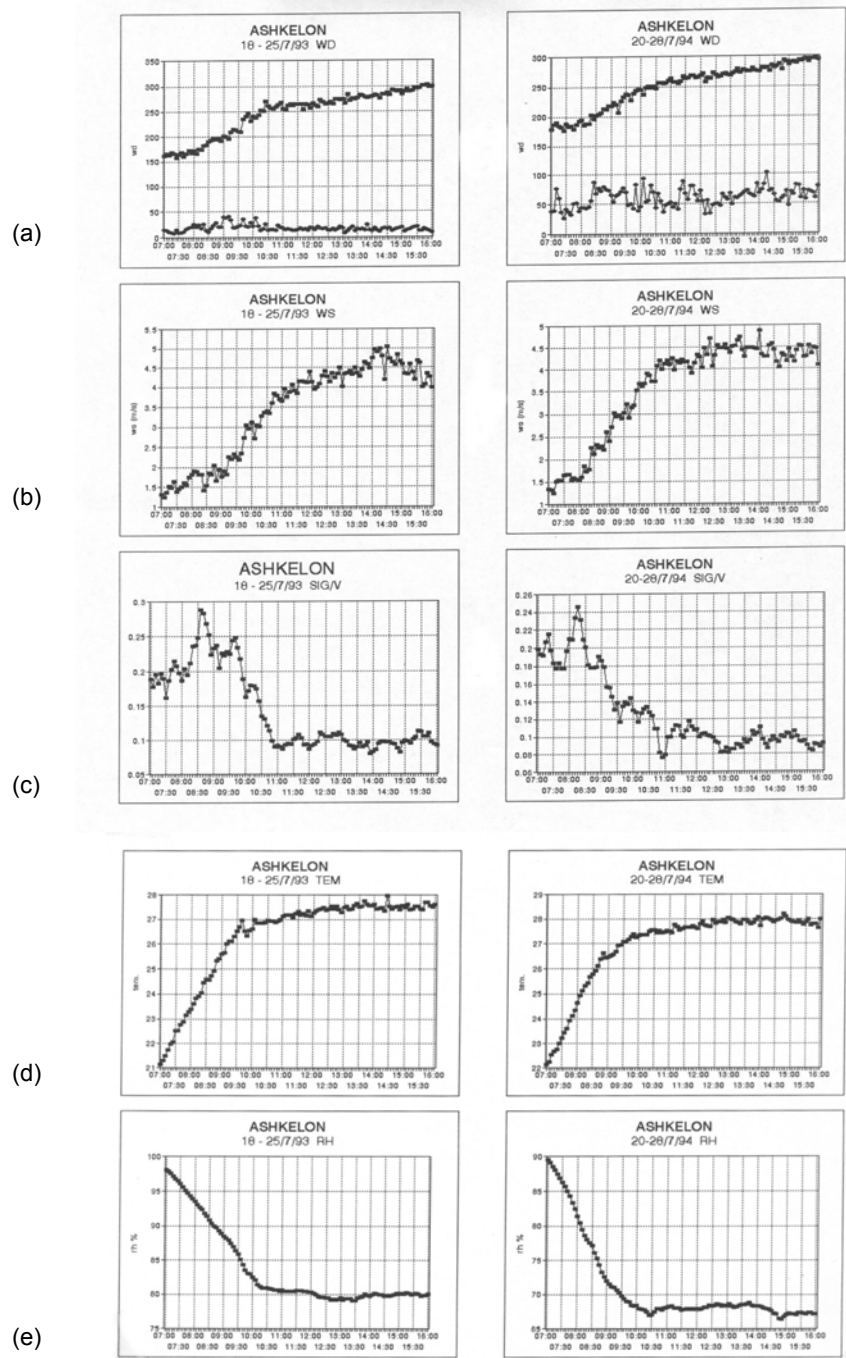
Figure 9a-e As in Fig. 2, but averaged for 18-25 July 1993 (left panel) and for 20-28 July 1994 (right panel). The fields are AVG5 for wind direction, WD (a); wind speed, WS (b); turbulence intensity, G (c); temperature, Tem (d) and relative humidity, RH (e).

REFERENCES

Alpert, P., Cohen, A., Neumann, J. & Doron, E. 1982: A model simulation of the summer circulation from the eastern Mediterranean past Lake Kinneret in the Jordan valley. *Mon. Wea. Rev.*, **110**, 994-1005.

Alpert, P., Kusuda, M. & Abe, N. 1984: Anticlockwise rotation, eccentricity and tilt angle of the wind hodograph, Part 2: Observational study. *J. Atmos. Sci.*, **41**, 3558-3573.

Alpert, P. & Eppel, E. 1985: A proposed index for mesoscale activity .*J. of Climate and Appl. Meteor.*, **24**, 472-480.

Alpert, P. & Getenio, B. 1988: One-level diagnostic modeling of mesoscale surface winds in complex terrain. Part I: Comparison with three-dimensional modeling in Israel. *Mon. Wea. Rev*., **116**, 2025-2046.

Alpert, P., Abramsky, R. & Neeman, B.U. 1992: The prevailing summer synoptic system in Israel - Subtropical high, not Persian trough. *Isr. J. Earth Sci.*, **39**, 93-102.

Arritt, R.W. 1993: Effects of the large-scale flow on characteristic features of the sea breeze. *J. Appl. Meteor.*, **32**, 116-125.

Atkinson, B.W. 1981: Mesoscale Atmospheric Circulation. Academic Press, London, 495pp.

Chiba, O. 1993: The turbulent characteristics in the lowest part of the sea breeze front in the atmospheric surface layer. *Bound. Lay. Meteor.*, **65**,.195-181

Clarke, R.H. 1955: Some observations and comments on the sea breeze. *Aust. Meteor. Mag.*, **11**, 47-52.

Doron, E. & Neumann, J. 1977: Land and mountain breezes with special attention to Israel's Mediterranean coast plain. *Israel Meteor. Res. Pap.*, **1**, 109-122, Israel Meteor. Service.

Estoque, M.A. 1962: The sea breeze as a function of the prevailing situation. *J. Atmos. Sci.*, **19**, 244-250.

Finkele, K., Hacker, J. M., Kraus H. & Byron-Scott, R. A. D., 1995: A complete sea-breeze circulation cell derived from aircraft observations. *Bound. Lay. Meteor.*, **73**, 299-317.

Fosberg, M.A. & Schroeder, M.J. 1966: Marine air penetration in central California. *J. Appl. Meteor.*, **5**, 573-589.

Geisler, J.E. & Bretherton, F.P. 1969: The sea-breeze forerunner. *J. Atmos. Sci.*, **26**, 82-95.

Glossary of Meteorology. 1959, Ed. By R.H. Huschke, American Meteor. Soc ,.Boston, 638pp.

Haurwitz, B. 1947: Comments on the sea-breeze circulation. *J. Meteor.*, **4**, 3-8.

Helmis, C.G., Asimakopoulos, D.N., Deligiorgi, D.G. & Lalas, D.P. 1987: Observations of sea breeze fronts near the shoreline. *Bound. Lay. Meteor.*, **38**, 395-410.

Kimble, G.H.T. 1946: Tropical land and sea breezes. *Bull. Amer. Meteor .Soc.*, **27**, 99-113.

Kusuda, M. & Alpert, P. 1983: Anticlockwise rotation of the wind hodograph. Part I: Theoretical study. *J. Atmos. Sci.*, **40**, 487-499.

Lyons, W.A. 1972: The climatology and prediction of the Chicago lake breeze. *J. Appl. Meteor.*, **11**, 1259-1270.

Lyons, W.A. & Olsson, L.E. 1973: Detailed mesometeorological studies of air pollution dispersion in the Chicago lake breeze. *Mon. Weather Rev.*, **1, 10**, 387-403.

Neumann, J. 1951: Land breezes and nocturnal thunderstorms. *J. Meteor.*, **8**, 60-67.

Neumann J. and Mahrer Y., 1971: A theoretical study of the land and sea breeze circulation. *J. Atmos. Sci.*, **28**, 532-542.

Neumann J. and Mahrer Y., 1974: A theoretical study of the sea and land breezes of circular islands. *J. Atmos. Sci.*, **31**, 2027-2039.

Neumann, J. 1977: On the rotation rate of the direction of sea and land breezes. . *J. Atmos. Sci.*, **34**, 1913-1917.

Orlanski, I. 1975: A rational subdivision of scales for atmospheric processes. *Bull. Amer. Soc.*, **56**, 529-530.

Pearce, 1955: The calculation of a sea breeze circulation in terms of the differential healing across the coast line. *Q. J. Roy. Meteor. Soc.*, **81**, 351-381.

Ramis, C., Jansa, A. & Alonso S., 1990: Sea breeze in Mallorca, A numerical study, *Meteor. Atmos. Phys.*, **42**, 249-258.

Rogers, R.R. & Yau, M.K., 1989: A short course in cloud physics. Pergamon Press, 293pp.

Schroeder, M.J., Fosberg, M.A., Cramer, O.P. & O'Dell, C.A. 1967: Marine air invasion of the Pacific coast: a problem analysis. *Bull. Amer. Meteor. Soc.*, **48**, 802-807.

Segal, M., Pielke, R.A., Mahrer, Y. & McNider, R.T. 1981: A numerical mesoscale model study of the pollutant mean trajectories during the warm season over central Israel - preliminary results. *Isr. J. Earth Sci.*, **30**, 1-1120

Segal, M., Mahrer, Y., Pielke, R.A. & Kessler, R.C. 1985: Model evaluation of the summer daytime induced flows over southern Israel. *Isr. J. Earth-Sci.*, **34**, 39-46.

Segal, M., Kallos, G., Brown, J. & Mandel, M. 1992: Morning temporal variations of shelter-level specific humidity. *J. Appl. Meteor.*, **31**, 74-85.

Segal, M. & Feingold, G. 1993: Impact of local convective cloud systems on summer day time shelter temperature. *J. Appl. Meteor.*, **32**, 1569-1578.

Sha, W., Kawamura, T. & Ueda, H., 1991: A numerical study on sea/land breeze as a gravity current; Kelvin-Holmholtz billows and inland penetration of the sea-breeze front. *J. Atmos. Sci.*, **48**, 1649-1665.

Simpson, J.E., 1964: Sea breeze front in Hampshire. *Weather*, **19**, 208-21.9

Simpson, J.E., Mansfield, D.A. & Milford, J.R. 1977: Inland penetration of sea breeze fronts. *Quart. J. Roy. Meteor. Soc.*, **103**, 47-76.

Simpson, J.E. 1994: Sea-breeze and Local Winds. Cambridge University Press. 228pp.

Skibin, D. & Hod, A. 1979: Subjective analysis of mesoscale flow patterns in northern Israel. *J. Appl. Meteor.*, **18,** 329-338.

Staley, D.O. 1957: The low-level sea breeze of northwest Washington. *J. Meteor.*, **14**, 458-470.

Wakimoto, R.M. & Atkins, N.T. 1994: Observations of the sea-breeze front during CaPE. Part 1: Single-Doppler, satellite and cloud photogrammetry analysis. *Mon. Weather Rev.*, **122**, 1092-1113.

Zambakas, J.D. 1973: The diurnal variation and duration of the sea-breeze at the national observatory of Athens, Greece. *Meteor .Mag.*, **102**, 224-228.